Journal of Materials Chemistry B

ROYAL SOCIETY OF CHEMISTRY

REVIEW

View Article Online
View Journal | View Issue

Cite this: J. Mater. Chem. B, 2023, 11, 9084

Virus-like particles nanoreactors: from catalysis towards bio-applications

Yuqing Su,†[a] Beibei Liu,†[a] Zhenkun Huang,†[a] Zihao Teng,[a] Liulin Yang,[b] Jie Zhu,[c] Shuaidong Huo*[a] and Aijie Liu*[a]

Received 15th May 2023,
Accepted 30th August 2023

DOI: 10.1039/d3tb01112g

rsc.li/materials-b

Virus-like particles (VLPs) are self-assembled supramolecular structures found in nature, often used for compartmentalization. Exploiting their inherent properties, including precise nanoscale structures, monodispersity, and high stability, these architectures have been widely used as nanocarriers to protect or enrich catalysts, facilitating catalytic reactions and avoiding interference from the bulk solutions. In this review, we summarize the current progress of virus-like particles (VLPs)-based nanoreactors. First, we briefly introduce the physicochemical properties of the most commonly used virus particles to understand their roles in catalytic reactions beyond the confined space. Next, we summarize the self-assembly of nanoreactors forming higher-order hierarchical structures, highlighting the emerging field of nanoreactors as artificial organelles and their potential biomedical applications. Finally, we discuss the current findings and future perspectives of VLPs-based nanoreactors.

1. Introduction

Organelles are essential compartments within living cells that sequester cargo materials and enzymatic reactions, to ensure controlled metabolic processes.[1] In nature, protein cage-based nanocompartments are commonly found in eukaryotes and prokaryotes.[2] These complex supramolecular systems are assembled from multiple copies of single or various protein monomers, providing a unique enclosed space for enzyme sequestration.[3] For instance, encapsulins, as bacterial organelle-like compartments, encompass one or more types of cargo proteins involved in diverse aspects of metabolism.[4] The intriguing features of organelles have motivated researchers to construct synthetic analogues, such as nanoreactors, using building blocks ranging from synthetic to biological materials.[5–7] Viral capsids have also been widely employed as nanocontainers and nanoreactors.[8] Viruses are particles that sequester and protect genetic materials from bulk environments and can release the genomes in the host cells. When the genomes are removed *in vitro*, diverse viral coat proteins can self-assemble and form virus-like particles (VLPs) with various sizes and morphologies.[9–12] To date, VLPs have been successfully utilized as physical barriers that protect catalysts or enhance their activity by enriching catalytic substances.[13] In this review, we will focus on VLPs-based nanoreactors. For other protein cage-based nanoreactors,[14,15] such as ferritin,[16–19] Lumazine synthetase (AaLS),[20–22] Encapsulins,[23,24] and *de novo* protein designs *et al.*,[25] we direct readers to recently reported review articles.[26–29]

Over the decades, VLPs-based nanoreactors have undergone significant advancements. VLPs are now recognized as versatile platforms that not only protect catalysts but also enable selective catalysis. The flux rates of reaction components can be altered owing to their intriguing physicochemical properties,[30,31] such as programmable pore sizes and surface charges. Additionally, the interior space of VLPs serves as an isolated reaction chamber,[32,33] allowing for simultaneous catalytic cascades when multiple populations of enzymes are encapsulated.[34,35] In addition to discrete particle-based nanoreactors, VLPs have also been utilized as building blocks to construct higher-order assemblies, spanning from two dimensions to three dimensions.[36,37] The uniform size and symmetrical structure of VLPs are beneficial for self-assembly. In general, the symmetrical arrangement of functional groups on the exterior surface of the capsid promotes the directed interactions between particles, resulting in the formation of ordered superstructures with lengths from the sub-micrometer to a few micrometers.[38,39] When these superlattice materials are composed of two populations of enzyme-packed VLP modules, two-step reactions with controllable catalytic activities can occur across multiple length scales and exhibit enhanced functions owing to closely packed building blocks.[40]

[a] Fujian Provincial Key Laboratory of Innovative Drug Target Research, School of Pharmaceutical Sciences, Xiamen University, Xiamen 361102, China. E-mail: aijieliu@xmu.edu.cn, huosd@xmu.edu.cn
[b] State Key Laboratory of Physical Chemistry of Solid Surface, Key Laboratory of Chemical Biology of Fujian Province, College of Chemistry and Chemical Engineering, Xiamen University, Xiamen 361005, P. R. China
[c] National-Local Joint Engineering Research and High-Quality Utilization, Changzhou University, Changzhou 213164, China
† These authors contributed equally.

More recently, research has gradually focused on utilizing these catalytically active nanocompartments as artificial organelles, and integrating designed catalytic reactions with living cells.[41] The purpose of this combination is to understand the metabolic network in living cells to correct dysfunctional processes or to introduce new orthogonal functions. One envisioned application is the development of a more sophisticated form of enzyme replacement therapy for the treatment of metabolic diseases. Beyond that, artificial organelles with functions such as stimulated activation of compounds (prodrugs) in target cells have been explored for selective anticancer treatment.[42] This provides a new strategy for future enzyme-prodrug therapies. In addition, the inherent advantages of VLPs endowed properties such as controlled self-assembly,[43–45] enhanced thermal stability[46,47] and customized multi-cargo encapsulation *et al.*,[48,49] have led to diverse applications such as biosensors and biodiagonstics.[50]

This review will summarize the recent advancements in VLPs-based nanoreactors. As shown in Fig. 1, we first discuss the physicochemical properties of the most commonly studied viral capsids, clarify the gating effects, and resulting selective catalytic activities. We will also show the advantages of encapsulating multiple populations of enzymes within VLPs, which enables cascade reactions within confined spaces and enhanced catalytic efficiencies. Furthermore, we will summarize the self-assembly of nanoreactors through various supramolecular interactions, leading to the formation of higher-order superstructures, and discuss the effects of hierarchical structures on catalytic kinetics. We will also explore the roles of VLPs-based nanoreactors in correcting defective cells for therapeutic purposes.[13] Finally, we will discuss the current findings and potential avenues for future studies to further harness the physicochemical properties of VLPs for applications in biomedicine.

2. Physicochemical properties of viral capsids and their impact on catalytic reactions

2.1 Physicochemical properties of viral capsids and construction of nanoreactors

During natural evolution, viruses have developed a wide variety of capsids to package, protect, and deliver their DNA or RNA genomes.[51–53] VLPs derived from viral structural proteins serve as prime examples of engineered nanoscale compartments. The inherent structural advantages of VLPs encompass the following key aspects: (1) highly ordered and self-assembling structure; (2) high surface area with patterned reactive groups facilitate precise anchoring of functional moieties in specific orientations;[54,55] (3) interior cavity is capable for efficient cargo encapsulation; (4) porous structures facilitate the exchange of chemical/materials with the bulk environment.[56] These distinctive properties collectively determine the promising potential of VLPs in the realm of catalysis. The following table presents the physicochemical properties of selected viral capsids, which have been extensively employed as nanoreactors for diverse applications in the field of catalysis and biomedicine (Table 1):

Some plant RNA viruses can undergo reversible disassembly and re-assembly *in vitro*, by varying the pH and ionic strength of the medium. One of the most extensively studied viruses in this category is cowpea chlorotic mottle virus (CCMV). This icosahedral virus is formed by 180 identical subunits of 20 kDa coat protein (CP), arranged around the RNA, forming a $T = 3$ capsid with an outer diameter of 28 nm and an inner diameter of 18 nm. Native CCMV particles are often stable under acidic pH and low ionic strength. Increasing the pH (>7.5) and the ionic strength (~ 1 M) causes electrostatic repulsion between protein subunits (due to the deprotonation of carboxyl groups). High

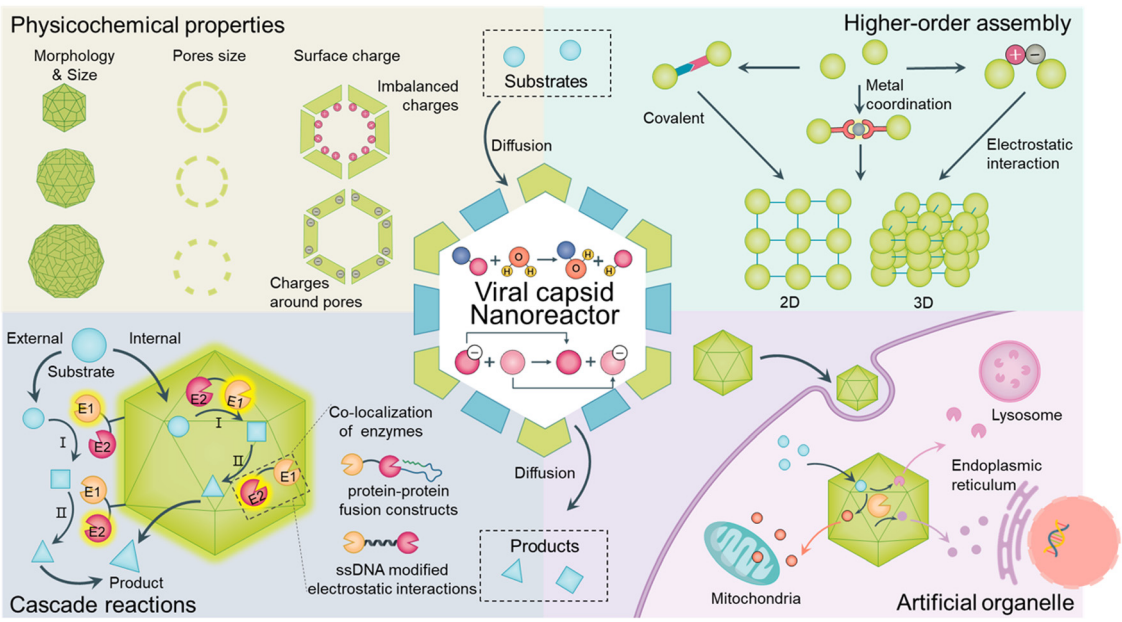

Fig. 1 Schematic overview of VLPs-based nanoreactors and their bio-applications.

Table 1 Relevant information on VLPs discussed in this review

Virus diameter (nm)	The triangulation number	Catalysts	Catalyst loading methods & advantages	Applications	Ref.
MS2	$T = 3$	TnaA + FMO	Electrostatic interactions	Encapsulation and co-localization multiple enzymes	34, 57
$D_{in} = 15$		Phosphatase	Efficient load of cargo	*In vivo*	
$D_{out} = 27$			Applicable to different cargo	Exploration of catalytic reaction process	
			Operation is simple and convenient		
P22	$T = 7$	AdhD	(DNA/RNA tags)	Studies of the substrate molecules in the catalytic reaction	58, 59
$D_{in} = 48–50$			Precise control of cargo load	New and stable nanocatalyst	
$D_{out} = 58–64$			Good biocompatibility and stability		
CCMV	$T = 3$	GOx/GCK	Biotin–streptavidin affinity interactions	Nanocompartments for catalytic reactions/cascade reactions	48, 60–62
$D_{in} = 18$		CYP	Control the bioactive molecules' orientation	Enzyme prodrug treatment	
$D_{out} = 28$		HRP			
		Au-NPs			
BMV	$T = 3$	GOX	Avoid enzyme deactivation and blocking of their active sites	Smart breast cancer therapy	63, 64
$D_{in} = 15$		GCase		Enzyme replacement therapy (ERT) for Gaucher's disease	
$D_{out} = 25$					
Qβ	$T = 7$	PepE	Immuno-assembly	Study in quantitative kinetic of enzymes in free *versus* protein-encapsulated	65
$D_{in} = 21$			High selectivity and specificity		
$D_{out} = 28$					
TMV	—	[SA]-GOD	Good biocompatibility and stability	Electrochemical biosensor	50, 66
$D_{in} = 4$		PQQ-GDH		Electrocatalytic system	
$D_{out} = 18$					
HBV	$T = 3$	yCD		Biosensing and drug delivery	40
$D_{in} = 22$					
$D_{out} = 32$					
SV40	$T = 3$	yCD	Protein fusions (SpyTag/SpyCatcher) (SrtA/SP)	Enzyme prodrug treatment	67
$D_{in} = 40$			Directional controlled load		
$D_{out} = 45–55$					
M13	—	HRP	Multi-functional load of different cargo	Intracellular delivery of protein orenzyme	68
$D_{in} = 2–4$			High structural stability and tolerance		
			hyaA/hyaB		
$D_{out} = 6–8$					

ionic strength also reduces the electrostatic interaction between protein units and RNA. Consequently, this results in the disassembly of the capsid. After removing RNA, purified CP subunits can self-assemble into empty capsids when the pH is lowered to 5.0.[43] Furthermore, similar pH-dependent assembly/disassembly behaviors are also observed in other icosahedral viruses, such as red clover necrotic mosaic virus (RCNMV) and brome mosaic virus (BMV).[63,69] This pH-dependent disassembly and reassembly behavior provides a straightforward method for the passive encapsulation of a diverse array of cargo.[70–72] Encapsulation of catalysts or enzymes through electrostatic interaction is another common approach. In this context, one should carefully consider the surface charges of the capsid, since the external surface charge may potentially disrupt the interactions between the capsid and cargo, further influencing the assembly process.[60,73] For instance, under neutral pH, the exterior surface of the CCMV capsid is slightly negatively charged while the inner surface is highly positively charged. This charge distribution character facilitates the encapsulation of negatively charged cargo, such as DNA tags or polystyrene sulfonate (PSS) modified enzymes,[74,75] anionic ligand functionalized gold nanoparticles,[76,77] *etc.* Encapsulation of enzymes can also be achieved through protein fusion. For example, Patterson *et al.* achieved encapsulation of alcohol dehydrogenase (AdhD) within *Salmonella typhimurium* phage P22 capsid by fusing AdhD to the N-terminus of the scaffolding protein (SP).[78] The P22 VLPs comprise 420 copies of a 46.6 kDa CP assembled into a $T = 7$ icosahedral capsids, aided by approximately 100–300 copies of scaffold protein (SP). Encapsulation of enzymes within VLPs contributes to improving their resistance to proteases and environmental stress. For instance, both CCMV and Qβ exhibited notable stability across a broad pH range (4–10) and at elevated temperatures (>75 °C),[79,80] consequently, improving the stability of the encapsulated enzymes through improved structural integrity and reduced enzyme-enzyme aggregations.[65]

In addition to the encapsulation of catalysts/enzymes within capsids, immobilization of catalysts/enzymes on the exterior surface of the VLP scaffolds has also been reported to enhance catalytic efficiencies, such as tobacco mosaic virus (TMV). The genome of TMV consists of a single-stranded RNA with 6395-nucleotides and approximately 2130 copies of CPs. TMV particles manifest as hollow cylinders with 300 nm in length, and external and internal diameters of 18 and 4 nm, respectively.[81]

The well-ordered functional amino acids on the exterior surface of TMV scaffolds endow with patterned immobilization of catalysts/enzymes, facilitating applications in biosensors,[66] online monitoring, and treatment.[50,82]

2.2 Dynamic capsid pores and molecular selectivity

Numerous studies have revealed the dynamic nature of viral structures, existing as ensembles of various states. The concept of "viral breathing" was introduced to describe the reversible alterations in the structural conformation of viral particles.[83] This dynamic fluctuation may be a general phenomenon among VLPs, given that coat proteins are assembled *via* non-covalent interactions by nature.[52] Perturbations at the protein–protein interfaces can induce various conformational changes, resulting in changes in pore sizes of capsid.[84]

To date, a spectrum of degrees of structural dynamics has been unveiled.[85–87] For example, Tama *et al.* employed the CCMV viral capsid as a model system to investigate the capsid dynamics, and elucidated the mechanism of pH-triggered breathing processes. The native state of CCMV remains stable around pH 5.0; however, the removal of Ca^{2+} or Mg^{2+} metal ions, or raising the pH (>6.5) causes a notable disruption of interactions at the quasi-3-fold interfaces, leading to a swollen state with substantial conformational changes.[84] Consequently, the average size of viral particles increases by approximately 10%, coupled with the enlargement of pore size from 1 nm to 2 nm,[88] as calculated from the Cryo-electron microscope (Cryo-EM) analysis.[89,90]

Apart from environmentally stimulated conformational changes, Brasch *et al.* observed that enzyme-loaded CCMV capsid with $T = 1$ icosahedral symmetry exists in two distinct classes, with sizes of 214 Å (class I) and 226 Å (class II).[48] The snapshots of Cryo-EM hinted a potential "breathing" motions of capsid in solution. However, the current study was unable to determine whether this arises from interconversion between the two states, or if various forms of capsid coexist in solution. Nonetheless, these breathing dynamics of capsid might be too subtle to discern through Cryo-EM. Selivanovitch *et al.* indicated that the effective pore sizes of P22 viral capsids may not coincide with the calculated result from Cryo-EM. In their work, the dynamic respiration of viral capsids was carried out by studying the diffusion rate of catalytic substrates across distinct P22 viral capsids.[58] As shown in Fig. 2a, alcohol dehydrogenases (AdhD) were encapsulated within the P22 VLPs, which displayed three types of morphologies: procapsid form (PC), expanded form (EX), and wiffle ball (WB), exhibiting pore sizes of approximately 4.2 × 1.9 nm, 2.3 × 1.5 nm and 10 nm. To study the gating effects of capsid pores, reaction species, such as nicotinamide adenine dinucleotide hydrogen (NADH) molecules were conjugated to six PAMAM dendrimers of various sizes. A linear response between the K_{cat} ratio and the increasing size of NADH-dendrimers indicates the presence of a soft (dynamic) barrier. Conversely, a rapid response implies a rigid

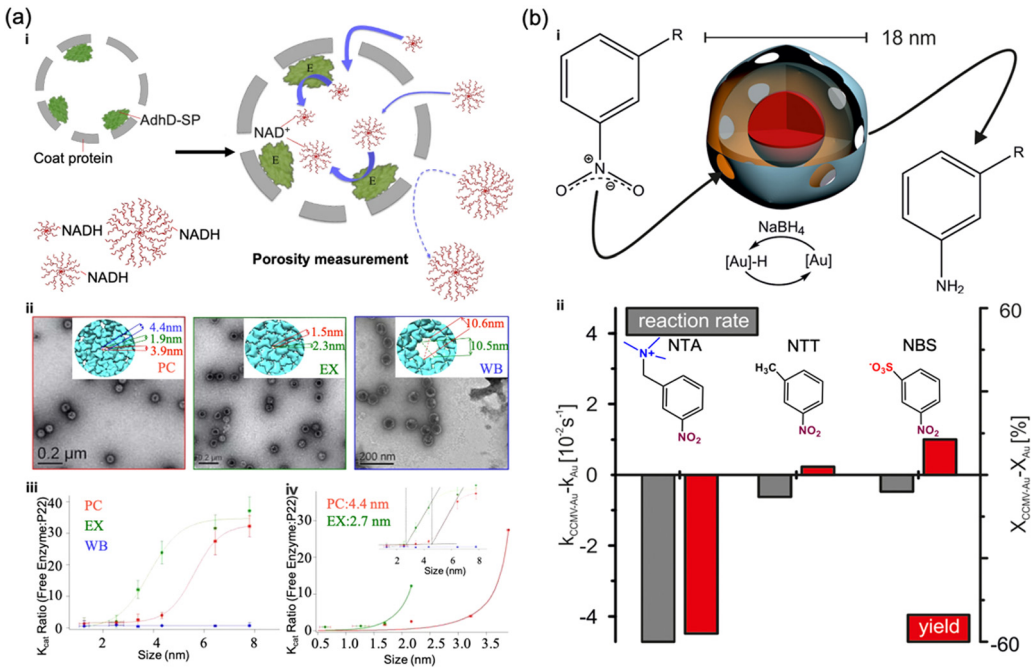

Fig. 2 (a) Enzymatic reactions and synthetic substrates of different sizes were used to detect the porosity of P22 VLPs with different morphologies. (PC, procapsid; EX, expanded; WB, wiffle ball). (i) The schematic diagram of the experiment; (ii) TEM of P22 VLP with different porosity; (iii) K_{cat} ratio using free enzyme and enzyme be encapsulated in PC, EX and WB; (iv) aqueous pore model fit of K_{cat} ratio data and estimated pore sizes for PC and EX. Figure adapted from ref. 58 with permission from Nature Portfolio, copyright 2021. (b) Gold nanoparticles encapsulated CCMV nanoreactors and catalyzed the reduction of nitroarenes with different substituents (NBS, NTT, NTA). (i) The schematic diagram of the experiment; (ii) reaction rates and yields of different substituents. Figure adapted from ref. 104 with permission from American Chemical Society, copyright 2016.

barrier. In this study, a linear relationship between the K_{cat} ratio and increasing molecular size was found, with the size limit falling within the range of 4.2–6.2 nm. This span surpasses the results calculated from Cryo-EM, suggesting that the P22 capsid may undergo dynamic breathing.

Collectively, the dynamic nature of pores could significantly affect the size threshold and diffusion rates of reaction species, and further influence the catalysis processes. Therefore, a deep understanding of the breathing dynamics of VLPs will be beneficial for the rational design and construction of nanoreactors. In addition to snapshots from cryo-EM analysis, integration of tools enabling time-resolved analysis, *e.g.*, time-resolved X-ray crystallography,[91,92] single-particle approaches,[93] *etc.*, can help to capture the potential intermediates. This approach aids to elucidate the dynamic pore structures and the underlying mechanisms governing viral breathing.

Furthermore, regarding the engineering of viral capsid pores for the purpose of constructing nanoreactors for biomedical applications,[94] several critical considerations emerge: (1) it is necessary to consider whether the pores' permeability aligns with the desired scope of chemical exchange.[95] Especially when the nanoreactors were integrated with complex living cells, it will be a great challenge to distinguish the desired substrates when they are in a mixture of compounds with similar physicochemical properties. The structural manipulation of pores can be mainly achieved by adjusting the capsid components or optimizing their topology.[85,96] For instance, Adamson *et al.* genetically engineered protein cages encompassing a broad spectrum of pore sizes and charges, thereby achieving control over molecular flux.[86] Chemical modification is also available, Gao *et al.* constructed protein cages with switchable permeability of O_2 by controlling the molecular patches on pores.[97] This innovation holds great potential in the applications of oxygen-sensitive catalysis and drug delivery. (2) Drawing inspiration from the natural (sub-) cellular membrane, an avenue worth exploring involves the integration of diverse functional components into the protein shells. For instance, membrane transport proteins, are known for their ability to sustain chemical gradients across cellular membranes.[98,99] In this context, pore engineering, coupled with stimuli-responsive molecules, could help to construct logic gates. This approach could effectively navigate the intricacies of handling intricate factors while enabling precise control over nanoreactor function.[100,101]

2.3 Surface charge of viral capsids can result in selective catalytic reactions

The electrostatic potential generated across the viral capsid can affect the diffusion of charged substrates, consequently, influence the overall catalytic rates. Therefore, obtaining a comprehensive understanding of the spatial arrangement of positive and/or negative charges throughout the entire capsid is necessary. In this context, Podgornik *et al.* performed an exhaustive of about 130 empty viral capsids,[102] unveiled that the capsid's charge distribution is a result of a combination of factors, such as surface charge densities, dipole moments, and geometric properties. Importantly, these characteristics can exhibit significant variations from virus to virus. For example, in the case of cucumber mosaic virus (CMV) capsids, the exterior and inner surfaces are positively and negatively charged, respectively. Whereas, simian virus 40 (SV40) capsids display a uniform distribution of mixed charges, instead of a division of charges between two distinct surface sides.[102]

For both native and engineered viral capsids, the surface charge densities can be determined by the electrostatic calculation based on the Poisson–Boltzmann theory. For instance, in the case of wild-type CCMV, the exterior surface of the capsid has a charge density less than 0.1 e nm^{-2}, while the inner surface has a charge density larger than 0.8 e nm^{-2}.[103] Studies have shown that the highly positively charged inner surface of the capsid significantly influences the diffusion of charged molecules and thus affects the catalytic pathways.[87] For example, in a study of nitroarene reduction using native-CCMV VLP-based nanoreactors, as shown in Fig. 2b, the catalytic rates for selected substrates were reduced due to the diffusion barrier of the protein shells.[104] However, this hindrance was more pronounced for positively charged nitroarene compared to neutral and negatively charged counterparts. This observation indicated the electrostatic potential generated across the capsid does affect the diffusion of charged substrates, consequently, modulating the overall catalytic rates. Furthermore, the catalytic reaction yield of negatively charged substrates exceeded that of neutral and positively charged substrates. This phenomenon might raise from the orientation of charged substrates within the confined charged space. However, it was noted that direct modification of charged functional groups at the molecular level might alter their electronic properties. It is particularly evident for aromatic molecules, where the mesomeric effect can play a significant role, possibly complicating the mechanistic studies. A universal method to study the effects of electrostatics on the diffusion of substrates across protein shells was introduced recently by Selivanovitch *et al.*[58] More specifically, the enzyme AdhD was encapsulated in P22 VLPs, and the substrate NADH was conjugated to dendrimers bearing neutral or negative charge. This approach eliminates the potential electronic effect and reveals the true impact of the electrostatic effect on substrate diffusion.

Genetic engineering of the charged residues around capsid pores can alter the electrostatic interactions between pores and reaction species. As a result, it finely adjusts the diffusion rates of charged substrates, thereby influencing the metabolic reactions and precisely modulating catalytic pathways. For instance, in the case of the MS2 capsids model system, mutants with increased negative ($MS2^{T71E}$ and $MS2^{T71E/V72D}$) or positive ($MS2^{T71K/V72R}$) charge around pores were generated to explore the coulombic effects on both charged substrate and product diffusion.[57] However, the local electric field not only influences the diffusion of charged species,[105–107] but also exerts an impact on the catalytic activity by lowering intermediate energies and activation barriers, leading to an enhanced electron transfer.[108,109] Genetic engineering emerges as a valuable tool for precise control over charge positioning and density.[105,110]

Harnessing such electrostatic guided processes, such as intermediate transport, enhanced electron transfer, *etc.*, will help to enhance the overall catalytic reactivity. A promising avenue is to synergize the benefits of molecular sorting and local electric fields modulated activities, which will offer a more comprehensive approach for achieving selective catalysis.

2.4 Local pH of viral capsid

The pH within the viral capsid can have a significant impact on the enzymatic reactions, thus necessitating precise evaluation.[111,112] Maassen *et al.* developed a strategy for interior pH probing by employing pH-responsive probes conjugated to negatively charged polymers, which were subsequently encapsulated in CCMV VLPs. Their findings revealed that the pH within the CCMV capsid is approximately 0.5 units more acidic than the surrounding bulk solution,[113] contributing to the Donnan potential across the viral capsid.

In a recent development, Muhren *et al.* confirmed the applicability of the Donnan theory in predicting the local pH shift through the utilization of the Poisson–Boltzmann theory.[114] Both theoretical analyses and experimental studies suggest that the immobile charges of amino acid residues on the surface of capsid can induce an imbalanced charge distribution. This disparity could potentially influence the influx of positively charged protons, consequently leading to pH shifts. In nature, protein cages such as carboxysome and Dps nanocages exhibit a more acidic local environment, thereby benefiting enzymatic catalytic activities.[107,112] In addition to the studies of pH in native VLPs, a comprehensive understanding of the physicochemical condition and personalized regulation of the local pH within viral capsids holds the potential to position VLPs as promising platforms for enhancing catalytic performance.[107,114]

3. Cascade reactions in VLPs-based nanoreactors

The cellular microenvironment of natural organisms is a complex network composed of a variety of enzymes. Under physiological conditions, different enzymes are located inside compartments or on the membrane to produce natural products with unparalleled synthetic efficiencies. Enzyme immobilization technologies have paved the way for cascade catalytic systems endowed with high stability and controllability.[115] A key element in controlling multistep reactions lies in the capability to govern the channeling of intermediates from one active site to the other, which can be achieved by using compartments or scaffolds with guided transport.[116] To date, VLPs have received extensive attention as multifunctional nanocarriers, demonstrating remarkable potential for facilitating cascade reactions. These reactions have shown profound advantages both within the viral cavities and along with the surface of the viral capsids.[117]

3.1 Cascade reactions within cavities of VLPs

Mimicking the cascade biochemical pathways within the confined intracellular space, VLPs serve as promising platforms where multiple enzymes are co-encapsulated. The capsid acts as a barrier, segregating the inner cavity from the external environment.[106] VLPs can enrich substrates within the cavity, restrain the random diffusion of intermediates, and reduce unnecessary interference from the bulk solution, resulting in enhanced intermolecular communication.[29] In addition, the enclosed enzymes benefit from better stability due to the constrained environment with reduced denaturation entropy.[115,118] The challenges of replicating the intracellular multienzyme cascade pathway in confined VLPs include co-localizing of distinct enzymes with designed stoichiometry and co-assembling diverse enzymes at specific distances to regulate the diffusion kinetics between active sites. To construct multienzyme within the same compartment, strategies such as electrostatic interaction and protein–protein fusion have been introduced, enabling them to work corporately within a specialized microenvironment.

Electrostatic interaction-directed encapsulating of enzymes has demonstrated high loading efficiency and a reduced chance of empty capsid formation, offering potential advantages for catalytic reactions. In this method, enzymes with tailored stoichiometry are coupled first, and the inter-space between enzymes is finely adjusted with the control of linker length. For example, Brasch *et al.* employed negatively charged DNA or polystyrene sulfonate for modifying and connecting two different enzymes. Subsequent encapsulation was achieved *via* electrostatic interactions between negatively charged moieties and positively charged coat proteins (Fig. 3a).[48] Although the wide versatility of this strategy has attracted interest from researchers, the potential issues also need to be taken into concern. For instance, surface modification of charged ligands may inadvertently attract or repel charged substrates, intermediates, and products, thereby influencing the overall catalytic rate.[56] Thus, a balanced amount of surface modification is needed to ensure high encapsulation efficiency along with highly enhanced cascade catalytic reactivity.

The protein–protein fusion strategy can spatially control various enzymes within confined VLPs. Zhang *et al.* constructed *Scheffersomyces stipitis* (SsCR) and a glucose dehydrogenase within P22 VLPs, the recycling efficiency of nicotinamide adenine dinucleotide phosphate (NADPH) was enhanced by a factor from 3 to 5 when multienzymes were encapsulated.[119] Notably, this system also exhibited enhanced stereoselectivity. The confinement effect was suggested to be attributed to altering the energy levels of transition states, thus resulting in enhanced chiral selectivity. However, the exact configuration of SsCR within P22 capsids remains partially understood, and the mechanism underlying enhanced stereoselectivity remains a subject for further study, an avenue ripe for future advancements in the development of cascade reactions.

Within a confined nanocompartment, co-localization of enzymes has been proposed to enhance the effective concentration of enzymes and intermediates, consequently, positively affecting the overall performance of the multienzyme system.[120] However, it is important to note that merely co-localization of multiple heterologous enzymes does not

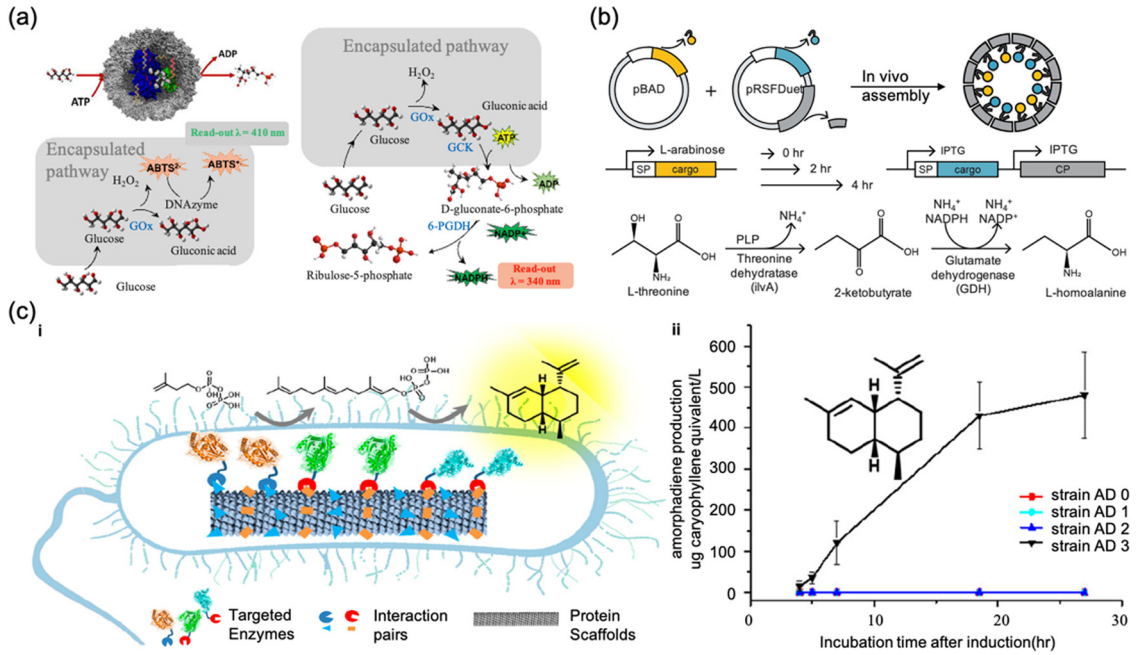

Fig. 3 (a) Two different glucose oxidase-based cascade systems were assembled using single-stranded DNA in the CCMV protein capsid and both showed enhanced catalytic activity. Figure adapted from ref. 48 with permission from American Chemical Society, copyright 2017. (b) *In vivo* co-localization of enzymes within P22 VLPs with stoichiometric control. Figure adapted from ref. 49 with permission from American Chemical Society, copyright 2023. (c) (i) A scaffold assembly based on the TMV multienzyme complex in *E. coli* presents one example of assembly-induced catalytic "turn-on" effect. (ii) Generation of the amorpha-4,11-diene titers of strains AD 0 to AD 3. Figure adapted from ref. 124 with permission from American Chemical Society, copyright 2020.

guarantee an increase in catalytic activity; instead, it is essential to ensure sufficient substrate channeling to boost the overall catalytic rate.[29] Moreover, excessive enzyme packing within the capsid could lead to overcrowding, potentially causing a decline in catalytic activity. For instance, McNeale *et al.* constructed a tunable strategy for *in vivo* co-localization of enzymes within P22 VLPs with stoichiometric control. That is, by co-expressing cargos and scaffold protein (SP) fusion together with coat protein (CP).[49] As shown in Fig. 3b, the loading densities of both enzymes were discovered to influence their activities. The overall catalytic activity was improved by increasing the amount of threonine dehydratase from the rate-limiting glutamate dehydrogenase. Indeed, theoretically, elevating the catalytic rate of the rate-limiting enzyme enhances the overall cascade reaction rate,[116] and increasing the quantity of the rate-limiting enzyme is more practically feasible. Interestingly, further increasing the enzyme loading density resulted in a negative impact on the catalytic activity, a consequence likely from the unfavorable steric effects hindering substrate access to the active sites.[115] Nevertheless, a systematic design of cascade reactions within the nanocompartment demands comprehensive consideration of kinetics as well as spatial arrangement of enzymes. Recently, Gopich introduced a straightforward framework to indicate if clustered enzymes can regulate the overall catalytic rate.[121] Specifically, in a two-step sequential reaction (assume that enzyme 1 and enzyme 2 are in equal number and uniformly dispersed), the ratio of the intrinsic and diffusion-controlled rates can evaluate whether it is worth the efforts to co-localization of enzymes within cages, $k_i/4\pi Da = k_iN_i/4\pi Da$ (where k_i is the intrinsic catalytic rate of enzyme i (=1, 2), N_i is the number of enzymes in one cluster, D is the diffusion coefficient of the substrates and intermediates, a is the radius of a cluster). If the diffusion rate significantly surpasses the intrinsic catalytic rate, $k_i/4\pi Da \ll 1$, the probability of substrate channeling is minimal. Consequently, the co-localization of enzymes within the nanocompartment wouldn't enhance the overall catalytic rate. Co-localization becomes effective when the reactions are diffusion-controlled or when the intrinsic catalytic rate is comparable to the diffusion rate ($k_i/4\pi Da \geq 1$). Detailed discussions regarding kinetics considerations for the rational design of enzyme cascades have been presented elsewhere.[115,116,121,122] For VLPs-based nanoreactors, optimizing the activity of cascade activities necessitates an in-depth understanding of the reaction mechanism and cascade kinetics.[116] Manipulating the overall catalytic rate can be achieved through capsid surface and pore engineering, given that the diffusion rate of substrates, the channeling of intermediate (*e.g.*, electrostatic guided transport),[115] and the dissociation and diffusion rates of products can be highly affected by electrostatic interactions, *etc.*[106,115,121,123]

3.2 Cascade reactions on the exterior surface of the VLP scaffolds

The design of cascade reactions extends beyond the confined cavity-based reactions but also encompasses the exterior surface of VLPs. In this context, enzymes are immobilized on the VLP scaffolds. Patterned functional groups on the exterior surface can also assist in directionally regulating enzyme

distribution, thereby facilitating cascade reactions. Additionally, the immobilization of enzymes onto the scaffold can help inhibit conformational changes during the catalysis and purification processes. As a consequence, it increases the catalytic lifetime and promoted enzyme reutilization,[125–128] holds substantial potential for applications in diagnostic assays and biosensors.[129]

Recently, Wei *et al.* regularly fixed three terpene synthases to the TMV-derived VLP scaffolds using site-specific covalent reactions between orthogonal reactive protein pairs (SpyCatcher/SpyTag and SnoopCatcher/SnoopTag), as shown in Fig. 3c.[124] This scaffold-supported multi-enzyme complex was further compartmentalized within the bacterial cell *Escherichia coli* to produce amorpha-4,11-diene, a key precursor of artemisinin. Interestingly, metabolic flux control with a ''switch-on'' mechanism was observed for the scaffold-assembled multi-enzyme system, while the unassembled strains yielded no product. This method is available to accommodate a variety of enzymes at high capacity. Although the complex interwoven metabolic network of the internal environment makes it difficult to describe the multi-enzyme kinetics, the overall performance surpasses the catalytic mechanism.

The advantages of surface immobilization of enzymes on the exterior surface of VLPs are distinct, multiple anchor sites with highly defined geometry are able to precisely control the assembly state.[130] Multilayered catalytic arrays are also feasible to enhance the catalytic activity and system sensibility,[128] particularly benefit the development of microfluidics and lab-on-a-chip devices.[126,127] However, some aspects demand thoughtful consideration during the rational design: (1) during the immobilization of enzymes, the crosslinkers' length might need to be regulated since rigid fixation can spatially restrict the enzyme conformation. Linkers with appropriate lengths enable dynamic conformational adjustments, providing more possibilities for dense decoration;[131] (2) unlike enzymes encapsulated within cavities, surface-immobilized enzymes contend with unrestricted intermediate diffusion. To solve this problem, the swing-arms mechanism has emerged as a strategy to facilitate substrate channeling.[132] Moreover, the exposed enzymes or catalysts are susceptible to potential poisoning by toxic substances within the complex intracellular environment;[133,134] (3) both encapsulation of enzymes in VLPs and surface immobilization of enzymes on scaffolds might be considered to prevent cross-inhibition between reaction species.[120] Although a preliminary study has been carried out by using P22 VLPs as scaffolds for dual-sided cascade reactions, the catalytic efficiency was only 22–77% in comparison to free enzymes.[135] Optimization of both internal and external modifications to have a balance between the diffusion rate of chemicals and the catalytic efficiencies of enzymes is necessary for enhanced catalysis.[116]

4. Catalytic reactions in higher-order assemblies of VLPs-based nanoreactors

Many biological examples show a controlled assembly of numerous building blocks assembled hierarchically across multiple length scales.[136–139] Although precise spatial control over individual compartments remains a significant challenge, the preliminary approach towards utilizing VLPs-based nanoreactors as building blocks for constructing higher-order dimensions has turned successful owing to their structural stability, pre-determined geometry, and interactions between subunits.[140] Currently, covalent crosslinking, electrostatic interaction, and metal–ligand coordination have been employed to construct two-dimensional (2D) or three-dimensional (3D) structures.[141] Non-covalent interactions can provide particular value for controlled self-assembly and ordered patterning, owing to their dynamic nature and inherent flexibility.[141–143] On the other hand, the covalently linked higher-order assemblies demonstrate enhanced stability.[144]

The higher-order assembly of VLP-based nanoreactors in terms of catalysis has also been explored in recent years.[138] For example, Liu *et al.* constructed 2D compartmental films by interfacial crosslinking of CCMV VLPs.[145] As shown in Fig. 4a, functional nanoparticles, such as gold, or biomolecular like horseradish peroxidase (HRP), were encapsulated within VLPs and crosslinked into thin films. This method not only facilitated the encapsulation of diverse cargos while preserving their functionalities, but also paved the way for numerous applications, such as early detection of disease.[146,147] Catalytic systems (*e.g.*, gold nanoparticles) assembled in this manner exhibited enhanced catalytic efficiency with improved signal-to-noise ratio, thus establishing a groundwork for utilizing 2D-assembled VLPs-based nanoreactors in the development of biosensors and biomedical materials.[148]

Moreover, the 3D-assembled nanoreactors have also been utilized for catalysis. For instance, Liljeström *et al.* harnessed electrostatic interactions to assemble HRP-encapsulated CCMV VLPs and avidin protein into heterogeneous crystals.[149] Remarkably, the catalytic activity of encapsulated cargo within the crystalline complex persisted, even comparable to free HPR. In another example, P22 encapsulating β-glucosidase was self-assembled into a condensed-phase material with high local concentration,[150] generating protein macromolecular framework (PMFs) that could be easily recovered and reused. Apart from providing an isolated environment for specific catalytic reactions, natural metabolic compartments can maintain effective communications across different organization levels, ranging from distinct subcellular domains to the entire organs, forming metabolic reaction networks.[151] Within these networks, diverse organelles can communicate by utilizing the products from one pathway as intermediates for another. This concept has been applied to investigate the possibility of cascade reactions within compartmentalized 3D superlattice.[40] As shown in Fig. 4b, Uchida *et al.* successfully transformed the structure of the assembled array into an ordered configuration with a face-centered cubic lattice. Negatively charged P22 VLPs and positively charged PAMAM dendrimers were self-assembled into higher-order superlattice materials containing two individually encapsulated enzymes. These super-lattices maintained coupled catalytic activity, facilitating a two-step reaction to produce isobutanol.[40] This study provides an essential step towards the bottom-up

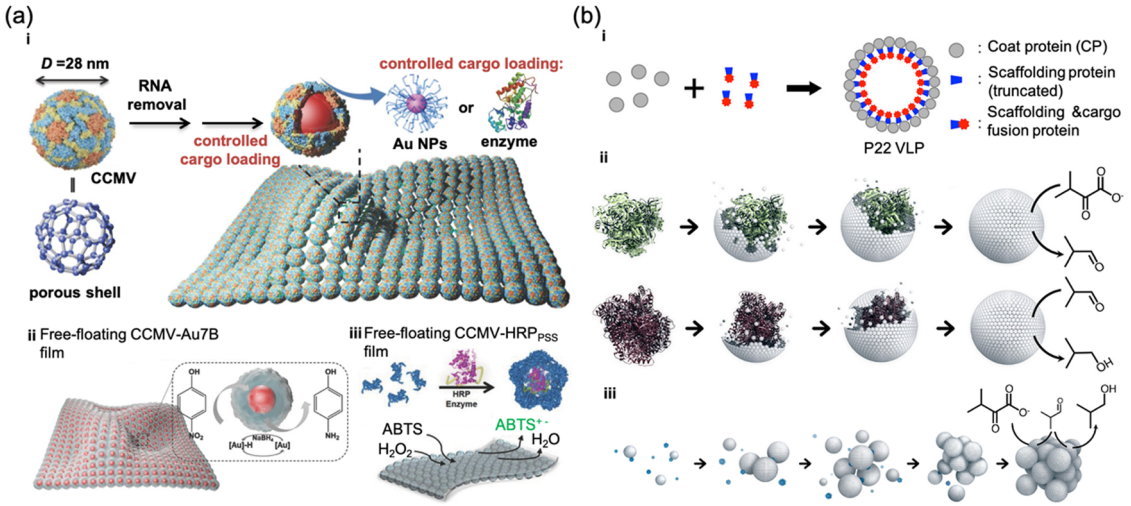

Fig. 4 (a) The gold NPs and the HRP encapsulated CCMV nanoreactors self-assembled into 2D thin films. (i) Schematic diagram of encapsulation strategy. (ii) Schematic illustration of the fabrication of a CCMV-Au7B-based free-standing film. (iii) Schematic illustration of the fabrication of CCMV-HRP$_{PSS}$ free-standing thin film. Figure adapted from ref. 145 with permission from Wiley-VCH GmbH, Weinheim, copyright 2018. (b) Schematic illustration of hierarchical self-assembly from protein subunit to a superlattice of catalytically VLPs. (i) Illustration of directed assembly of a P22 VLP with encapsulated cargo. (ii) Individual CPs self-assemble to form a VLP, templated by different SP-cargo fusion proteins. (iii) VLPs self-assemble into higher-ordered superlattice materials, mediated by positively charged PAMAM dendrimers (blue). Figure adapted from ref. 40 with permission from American Chemical Society, copyright 2018.

fabrication of functional superlattice materials using a self-assembly process across multiple length scales. Although current studies have been applying these higher-ordered assemblies of VLPs-based nanoreactors for industrial catalysis applications,[137] there has also been an extensive exploration of 3D assembly involving non-VLP-based protein cages for biomedical applications. One notable example is the formation of metal–organic frameworks (MOFs) through the coordination of nickel ions with bisH-SF, which triggers the self-assembly of ferritin nanocages. The constructed MOFs exhibit exceptional abilities in absorbing iron ions.[152] This property can be harnessed in the decomposition of H_2O_2 molecules to generate toxic hydroxyl radicals, holding tremendous potential for catalytic tumor therapy.[153] Similarly, utilizing the 3D network from protein-cages assembly demonstrates promise in stabilizing enzymes and protecting them from digestion.[154] This capability holds significant potential for *in vivo* catalytic applications. These studies ignite the possibility of utilizing 3D-assembled VLPs-based nanoreactors for catalytic therapy and biosensors.

5. Potential applications of VLPs-based nanoreactors in biomedicine

Biomedical utility has always been one of the focuses of VLP structural engineering. Their advantages lie in their inherent biophysical structure and the flexibility of modifications, which researchers have exploited successfully. VLPs-based nanoreactors constructed from these structures have been designed to perform selective catalytic activities, leading to the development of catalytic biomaterials at various length scales.[155] More excitingly, they have shown tremendous promise for biomedical applications, owing to their versatility, high stability, and biosafety. To this end, both genetic and chemical methods have been employed for targeting specific cells, prolonging blood circulatory half-life,[156,157] avoiding protease degradation, and escaping immune detection. VLPs-based nanoreactors have been utilized to integrate with living cells to restore lost functions or to introduce new functions into living cells for enzyme replacement therapy (ERT);[157] they have also shown profound potential for targeted cancer cells chemotherapy *via* enzyme prodrug activation (EPT).[63]

A variety of studies have demonstrated that VLPs-based nanoreactors can successfully replicate the role of metabolic enzymes for ERT.[158,159] As shown in Fig. 5a, to enhance the stability of enzymes in blood demands periodic intravenous administration, Chauhan *et al.* encapsulated the enzyme β-glucocerebrosidase (GCase) within VLPs derived from the BMV,[64] for the treatment of Gaucher disease, a common lysosomal disease arising from GCase deficiency. Notably, surface functionalization of the specific receptor is a widely used strategy for precise targeting.[160] Here, polyethylene glycol (PEG) modification helped to reduce non-specific cell interactions, and prolonged the blood circulation half-life of nanoreactors *in vivo*, promoting the uptake probability by the targeted cells. The terminal conjugation with mannose receptors further enhanced the internalization into macrophages, while bare BMV VLPs exhibited a broad biodistribution across various cell lines, including fibroblast, kidney, and hepatocytes.[159] It is worth noting that, viral capsid protection led to an approximately 11-fold enhancement in enzyme stability under the physiological conditions, implying a potential for reducing the requirement of multiple intravenous injections. Although to what extent the frequency can be reduced remains to be

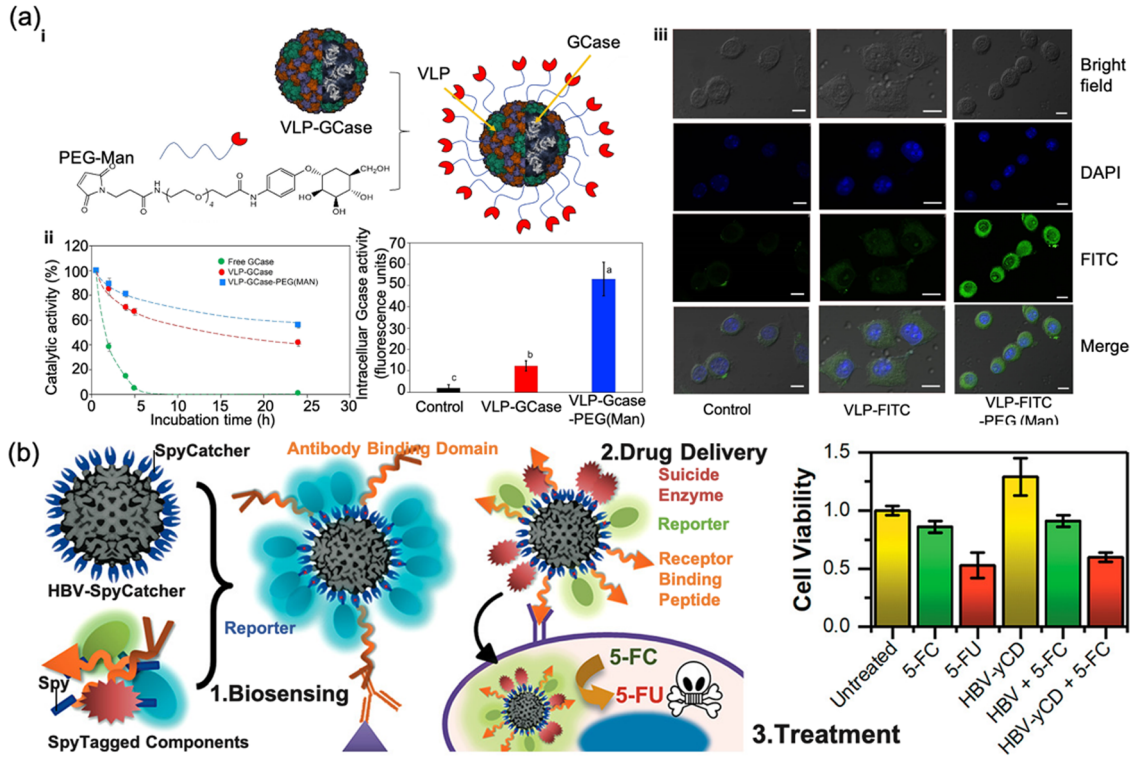

Fig. 5 (a) GCase is encapsulated within BMV and functionalized with a mannose group on its surface to target macrophages. (i) The synthesis of targeted enzymatic VLP-nanoreactors. (ii) Comparison of enzyme-catalyzed activity of VLP-GCase at different pH and in cells before and after functionalization. (iii) The priority uptake of functionalized VLPs cells was demonstrated by confocal microscopy. Figure adapted from ref. 64 with permission from Chemistry Europe, copyright 2022. (b) A powerful and highly modular HBV based smart nanodevice, this platform exhibits flexibility for biosensing and delivery of anticancer enzymes for prodrug activation. Figure adapted from ref. 164 with permission from American Chemical Society, copyright 2020.

explored,[161] this work indicates that VLPs-based nanoreactors are promising cost-effective alternatives for ERT.

In addition to ERT, VLPs-based enzymatic prodrug activation therapy (EPT) has also emerged as a promising tool to enhance cancer chemotherapy.[42,162] Presently, chemotherapy remains a prominent strategy for cancer treatment. However, limitations are also apparent, it can cause drug resistance and severe side effects. Most chemotherapeutic agents can be used as prodrugs and require activation to exert profound effects on cancer cells.[163] Therefore, enzyme prodrug therapy (EPT) has been employed for targeted activation of chemotherapies in diseased tissues.[56]

An early example described converting the chemotherapeutic drug 5-fluorocytosine (5-FC) to cytotoxic 5-fluorouracil (5-FU) to induce renal fibroblast cell (CV-1 line) death by using cytosine deaminase encapsulated SV40 VLP nanoreactors.[67] A more robust smart nanosystem for targeted activation of 5-FC was reported recently by Hartzell *et al.*[164] As shown in Fig. 5b, Hepatitis B virus-like particles (HBV VLPs) were used as modular nanocarrier platforms, here SpyCatcher/SpyTag were used for site-specific bioconjugation, endowed increased targeting avidity with efficient EPT for cancer cell killing. In fact, this "plug and play" protein pair enables the attachment of a wide range of functional moieties with high capacity. This strategy also showed significant signal amplification when applied for biosensing, with over a 1500-fold increase, enabling the detection of low nanomolar thrombin concentration with the naked eye. In another instance, DePorter *et al.* developed a nanoreactor for prodrug activation by displaying enzymes on the exterior of the bacteria phage M13-derived VLPs for prostate cancer cell treatment. Enhanced cell recognition and penetration were achieved by genetically fusing 12-amino acid peptide Ypep. Additionally, biotinylated phages were also introduced for chemical conjugation with HRP to oxidize the prodrug indole-3-acetic acid *in situ*, generating peroxyl radicals for cancer cell destruction.[68] Moreover, combining therapies have also been explored, Chauhan *et al.* encapsulated cytochrome P450 in the P22 VLPs to form a biocompatible nanoreactor; both photosensitizer and estrogen receptor (ER+) targeted species were modified on the exterior of capsid to perform both EPT and photodynamic therapy (PDT) for the treatment ER+ breast cancer.[165]

Collectively, chemical modification and genetic engineering techniques have endowed VLPs-based nanoreactors with multifunctions for wide biomedical applications.[166] Although VLPs-based nanoreactors hold significant potential for *in vivo* therapy, several considerations must be addressed prior to clinical applications: (1) enhancement of targeting efficiency: to further optimize VLPs-based nanoreactors for *in vivo* application, the overall targeting efficiency remains to be improved. Increasing the expression of specific receptors *via* gene editing is one of the strategies to enhance bioavailability; (2) ensuring long-term

stability: guaranteeing the sustained stability of VLPs-based nanoreactors over prolonged periods should be ensured so that nanoreactors can maintain their functionality within the required timeframe. Strategies such as elastin-like polypeptide (ELP) tag-modified CCMV have shown enhanced stability in a physiological environment.[167] However, various crucial factors remain unknown, *e.g.*, it is unknown to what extent the capsid degrades, how it affects enzyme activity and how the host responds to the released enzyme. The interactions with the major histocompatibility complex should be prevented, as this may lead to an immune response due to the recognition of foreign structures. Moreover, it will be interesting to study whether ELP-CCMV can also enhance enzyme stability against thermal stress; (3) preventing immune activation: when employing bacteriophage as a nanoreactor scaffold, the potential containment of bacterial lipopolysaccharide (LPS) must be addressed to avert immune activation.[168] Therefore, careful protein purification may be necessary before *in vivo* applications; (4) optimizing EPT: regarding the EPT application, concerted efforts must be taken to optimize the efficient transformation of diverse substrates, insights gleaned from the studies by Comellas-Aragones *et al.*,[61] Cardinale *et al.*[169] and Patterson *et al.*;[170] (5) balancing kinetic parameters when integration: it is important to balance the kinetic parameters so to better internalize with the metabolic network of the host cells. Although it is a great challenge, comprehensive kinetic analysis may be required since nanoreactors' behavior can diverge significantly between extracellular and intracellular environments, since the latter is much more crowded and complex.[56,171] (6) Expanding biomedical applications: integrating multi-function building blocks with VLPs-based nanoreactors may help to expand biomedical applications beyond ERT and EPT. For example, combining specific biomarkers that can be used for early disease diagnosis and progression monitoring with high sensitivity and specificity would benefit disease diagnosis and treatment. Overall, the use of VLPs as platforms for delivering deficient enzymes for therapeutic treatment is a rapidly growing area of research.

6. Summary and outlooks

One of the defining features of life is the compartmentalization of molecules. Physical boundaries effectively separate intricate metabolic processes from the complex external cellular milieu. Mirroring nature, researchers have prolifically developed nanoreactors in recent decades. The unique properties of virus-like particles (VLPs), including their highly ordered structures, stability, biocompatibility, and tunable assembly-disassembly properties, have spurred significant progress in engineering VLPs-based nanoreactors.

In this review, we summarize the latest accomplishments in nanoreactors across various scales and their prospective applications in biomedicine. Coupling VLPs with catalytic reactions extends benefits beyond improving catalytic stability and longevity.[172] The distinct physicochemical properties of viral capsids allow precise control over the entry and exit of substrates and products, thus influencing reaction pathways. Mimicking natural organelles, the spatial arrangement of multiple enzymes in restricted spaces has been harnessed to limit the diffusion of chemical intermediates, fostering enhanced interplay between enzymes. Beyond executing intricate reactions within single nanocompartments, chemical interactions can also transpire between different compartments when VLPs are closely packed. Furthermore, we also highlight recent developments and applications of nanoreactors in therapeutic interventions.

While extant research suggested promising potential for VLPs-based nanoreactors in biomedical applications,[173] several avenues demand further exploration. An intriguing direction is the conceptualization and assembly of VLPs-based nanoreactors as synthetic organelles for therapeutic purposes. Further fundamental studies should be carried out to construct nanoreactors with innovative functions, such as modulating the chemical environment (*e.g.*, pH, ionic conditions) or devising adaptable gates for refined substrate selectivity, to achieve ''on-demand control''.[174] Employing theoretical modeling and artificial intelligence in research could spotlight salient properties through data-driven inquiries.[175] Furthermore, the exploration of complex metabolic pathways within hierarchical assemblies of combined nanoreactors remains nascent. For instance, Wgghwani *et al.* proposed a nested protein cage system showcasing cell-like features by co-packaging ferritin cages and enzyme macromolecules within the P22 capsid.[176] Further extending the intricacy of higher-ordered hierarchical assemblies could provide deeper insights into communication channels and chemical signaling observed in natural living cells.[173]

Desired advancements also encompass precise control over *in situ* diagnosis and treatment. Numerous studies are already delving into the integration of functional elements, such as quantum dots,[177] magnetic particles,[178] and fluorescent entities,[177] within VLPs or on their surfaces for real-time, non-invasive bio-imaging.[178] The convergence of nanoreactors and bioimaging might pave the way for heightened disease diagnosis and treatment precision. Ideally, this could be done *via* a further combination of in-situ monitoring of metabolites with exceptional specificity and sensitivity, thus adjusting the activity of nanoreactors to enhance the therapeutic efficiency with minimized side effects. Meanwhile, comprehensive investigations into the pharmacokinetics, biodistribution, and immunogenicity of VLPs-based nanoreactors and their hybrids are imperative for bio-safety assurances.[179]

In summary, continuous efforts are required to unveil the full potential of VLPs-based nanoreactors. Rational structural design, coupled with an in-depth understanding of metabolic networks simulations and chemical signaling within and between nanocompartments, as well as at the interface between nanoreactor and living cells, will undoubtedly promote the development of nanoreactors. Through exhaustive ''whole-cell'' simulation and *in vivo* examinations, we anticipate that VLPs-based nanoreactors are expanding their application scope in biomedicine considerably.

Conflicts of interest

There are no conflicts to declare.

Acknowledgements

This work was supported by the National Natural Science Foundation of China (NSFC) (grant no. 22278040; no. 22302164), Fujian Provincial Department of Science and Technology (grant no. 2023J05014) and Xiamen Municipal Bureau of Science and Technology (grant no. 3502Z20227004). S. H. and A. L. are grateful for financial support from the Nanqiang Outstanding Young Talents Program from Xiamen University. A. L. would also like to thank Prof. Jeroen J. L. M. Cornelissen (University of Twente) and Prof. Feng Li (Wuhan Institute of Virology, CAS) for their discussions.

Notes and references

1 C. A. McHugh, J. Fontana, D. Nemecek, N. Cheng, A. A. Aksyuk, J. B. Heymann, D. C. Winkler, A. S. Lam, J. S. Wall, A. C. Steven and E. Hoiczyk, *EMBO J.*, 2014, **33**, 1896–1911.
2 D. Goel and S. Sinha, *Nano Express*, 2021, **2**, 042001.
3 E. C. Theil, *Inorg. Chem.*, 2013, **52**, 12223–12233.
4 T. W. Giessen and P. A. Silver, *Nat. Microbiol.*, 2017, **2**, 17029.
5 D. M. Vriezema, M. Comellas Aragonès, J. A. A. W. Elemans, J. J. L. M. Cornelissen, A. E. Rowan and R. J. M. Nolte, *Chem. Rev.*, 2005, **105**, 1445–1490.
6 R. Divine, H. V. Dang, G. Ueda, J. A. Fallas, I. Vulovic, W. Sheffler, S. Saini, Y. T. Zhao, I. X. Raj, P. A. Morawski, M. F. Jennewein, L. J. Homad, Y.-H. Wan, M. R. Tooley, F. Seeger, A. Etemadi, M. L. Fahning, J. Lazarovits, A. Roederer, A. C. Walls, L. Stewart, M. Mazloomi, N. P. King, D. J. Campbell, A. T. McGuire, L. Stamatatos, H. Ruohola-Baker, J. Mathieu, D. Veesler and D. Baker, *Science*, 2021, **372**, eabd9994.
7 H. Ren, S. Zhu and G. Zheng, *Int. J. Mol. Sci.*, 2019, **20**, 592.
8 J. Zhang, W. Zhang, M. Yang, W. Zhu, M. Li, A. Liang, H. Zhang, T. Fang, X.-E. Zhang and F. Li, *Nanoscale*, 2021, **13**, 11334–11342.
9 T. Douglas and M. Young, *Science*, 2006, **312**, 873–875.
10 M. Fischlechner and E. Donath, *Angew. Chem., Int. Ed.*, 2007, **46**, 3184–3193.
11 M. Uchida, M. T. Klem, M. Allen, P. Suci, M. Flenniken, E. Gillitzer, Z. Varpness, L. O. Liepold, M. Young and T. Douglas, *Adv. Mater.*, 2007, **19**, 1025–1042.
12 M. J. Rohovie, M. Nagasawa and J. R. Swartz, *Bioeng. Transl. Med.*, 2017, **2**, 43–57.
13 S. B. P. E. Timmermans and J. C. M. van Hest, *Curr. Opin. Colloid Interface Sci.*, 2018, **35**, 26–35.
14 K. Renggli, N. Sauter, M. Rother, M. G. Nussbaumer, R. Urbani, T. Pfohl and N. Bruns, *Polym. Chem.*, 2017, **8**, 2133–2136.
15 K. Renggli, M. G. Nussbaumer, R. Urbani, T. Pfohl and N. Bruns, *Angew. Chem., Int. Ed.*, 2014, **53**, 1443–1447.
16 S. Kanbak-Aksu, M. Nahid Hasan, W. R. Hagen, F. Hollmann, D. Sordi, R. A. Sheldon and I. W. C. E. Arends, *Chem. Commun.*, 2012, **48**, 5745–5747.
17 J. Zang, H. Chen, G. Zhao, F. Wang and F. Ren, *Crit. Rev. Food Sci. Nutr.*, 2017, **57**, 3673–3683.
18 K. W. Pulsipher, S. Honig, S. Deng and I. J. Dmochowski, *J. Inorg. Biochem.*, 2017, **174**, 169–176.
19 C. R. Olsen, T. J. Smith, J. S. Embley, J. H. Maxfield, K. R. Hansen, J. R. Peterson, A. M. Henrichsen, S. D. Erickson, D. C. Buck, J. S. Colton and R. K. Watt, *Nanotechnology*, 2017, **28**, 195601.
20 B. Wörsdörfer, Z. Pianowski and D. Hilvert, *J. Am. Chem. Soc.*, 2012, **134**, 909–911.
21 R. Frey, T. Hayashi and D. Hilvert, *Chem. Commun.*, 2016, **52**, 10423–10426.
22 Y. Azuma, R. Zschoche, M. Tinzl and D. Hilvert, *Angew. Chem., Int. Ed.*, 2016, **55**, 1531–1534.
23 Y. H. Lau, T. W. Giessen, W. J. Altenburg and P. A. Silver, *Nat. Commun.*, 2018, **9**, 1311.
24 F. Sigmund, C. Massner, P. Erdmann, A. Stelzl, H. Rolbieski, M. Desai, S. Bricault, T. P. Wörner, J. Snijder, A. Geerlof, H. Fuchs, M. Hrabe de Angelis, A. J. R. Heck, A. Jasanoff, V. Ntziachristos, J. Plitzko and G. G. Westmeyer, *Nat. Commun.*, 2018, **9**, 1990.
25 H. Li, G. Zheng and S. Zhu, *Microb. Cell Fact.*, 2018, **17**, 26.
26 J. M. Rodríguez, C. Allende-Ballestero, J. J. L. M. Cornelissen and J. R. Castón, *Nanomaterials*, 2021, **11**, 1467.
27 K. Renggli, P. Baumann, K. Langowska, O. Onaca, N. Bruns and W. Meier, *Adv. Funct. Mater.*, 2011, **21**, 1241–1259.
28 A. Mohanty, A. Parida, R. K. Raut and R. K. Behera, *ACS Bio Med. Chem. Au*, 2022, **2**, 258–281.
29 Y. Wang and T. Douglas, *J. Mater. Chem. B*, 2023, **11**, 3567–3578.
30 L. Schoonen, S. Maassen, R. J. M. Nolte and J. C. M. van Hest, *Biomacromolecules*, 2017, **18**, 3492–3497.
31 J. W. Wilkerson, S.-O. Yang, P. J. Funk, S. K. Stanley and B. C. Bundy, *New Biotechnol.*, 2018, **44**, 59–63.
32 J. Zhu, K. Yang, A. Liu, X. Lu, L. Yang and Q. Zhao, *Protein Expression Purif.*, 2020, **174**, 105679.
33 J. Zhu, X. Lu, Y. Li, T. Li, L. Yang, K. Yang, L. Ji, M. Lu and M. Li, *Catal. Lett.*, 2020, **150**, 3542–3552.
34 T. W. Giessen and P. A. Silver, *ChemBioChem*, 2016, **17**, 1931–1935.
35 D. Patterson, E. Edwards and T. Douglas, *Isr. J. Chem.*, 2015, **55**, 96–101.
36 G. Yang, L. Wu, G. Chen and M. Jiang, *Chem. Commun.*, 2016, **52**, 10595–10605.
37 A. Korpi, E. Anaya-Plaza, S. Välimäki and M. Kostiainen, *Wiley Interdiscip. Rev.: Nanomed. Nanobiotechnol.*, 2020, **12**, e1578.
38 M. A. Kostiainen, P. Hiekkataipale, A. Laiho, V. Lemieux, J. Seitsonen, J. Ruokolainen and P. Ceci, *Nat. Nanotechnol.*, 2013, **8**, 52–56.
39 S. Chakraborti, A. Korpi, M. Kumar, P. Stępień, M. A. Kostiainen and J. G. Heddle, *Nano Lett.*, 2019, **19**, 3918–3924.

40 M. Uchida, K. McCoy, M. Fukuto, L. Yang, H. Yoshimura, H. M. Miettinen, B. LaFrance, D. P. Patterson, B. Schwarz, J. A. Karty, P. E. Prevelige, Jr., B. Lee and T. Douglas, *ACS Nano*, 2018, **12**, 942–953.
41 R. A. J. F. Oerlemans, S. B. P. E. Timmermans and J. C. M. van Hest, *ChemBioChem*, 2021, **22**, 2051–2078.
42 J. F. Mukerabigwi, Z. Ge and K. Kataoka, *Chem. – Eur. J.*, 2018, **24**, 15706–15724.
43 J. E. Johnson and J. A. Speir, *J. Mol. Biol.*, 1997, **269**, 665–675.
44 B. J. M. Verduin, *J. Gen. Virol.*, 1978, **39**, 131–147.
45 W. Zhu, T. Fang, W. Zhang, A. Liang, H. Zhang, Z.-P. Zhang, X.-E. Zhang and F. Li, *Nanoscale*, 2021, **13**, 4634–4643.
46 J. D. Fiedler, M. R. Fishman, S. D. Brown, J. Lau and M. G. Finn, *Biomacromolecules*, 2018, **19**, 3945–3957.
47 S. Das, L. Zhao, K. Elofson and M. G. Finn, *Biochem.*, 2020, **59**, 2870–2881.
48 M. Brasch, R. M. Putri, M. V. de Ruiter, D. Luque, M. S. T. Koay, J. R. Castón and J. J. L. M. Cornelissen, *J. Am. Chem. Soc.*, 2017, **139**, 1512–1519.
49 D. McNeale, L. Esquirol, S. Okada, S. Strampel, N. Dashti, B. Rehm, T. Douglas, C. Vickers and F. Sainsbury, *ACS Appl. Mater. Interfaces*, 2023, **15**, 17705–17715.
50 C. Koch, A. Poghossian, C. Wege and M. J. Schöning, *In Virus-Derived Nanoparticles for Advanced Technologies: Methods and Protocols*, 2018, **1776**, 53–568.
51 M. G. Mateu, *Protein Eng. Nanostruct.*, 2016, **940**, 83–120.
52 J. D. Perlmutter and M. F. Hagan, *Annu. Rev. Phys. Chem.*, 2015, **66**, 217–239.
53 M. G. Mateu, *Arch. Biochem. Biophys.*, 2013, **531**, 65–79.
54 Y. Ma, R. J. M. Nolte and J. J. L. M. Cornelissen, *Adv. Drug Delivery Rev.*, 2012, **64**, 811–825.
55 E. Strable and M. G. Finn, *Curr. Top. Microbiol. Immunol.*, 2009, **327**, 1–21.
56 R. Koyani, J. Pérez-Robles, R. D. Cadena-Nava and R. Vazquez-Duhalt, *Nanotechnol. Rev.*, 2017, **6**, 405–419.
57 J. E. Glasgow, M. A. Asensio, C. M. Jakobson, M. B. Francis and D. Tullman-Ercek, *ACS Synth. Biol.*, 2015, **4**, 1011–1019.
58 E. Selivanovitch, B. LaFrance and T. Douglas, *Nat. Commun.*, 2021, **12**, 2903.
59 P. C. Jordan, D. P. Patterson, K. N. Saboda, E. J. Edwards, H. M. Miettinen, G. Basu, M. C. Thielges and T. Douglas, *Nat. Chem.*, 2016, **8**, 179–185.
60 L. Sánchez-Sánchez, R. D. Cadena-Nava, L. A. Palomares, J. Ruiz-Garcia, M. S. T. Koay, J. J. M. T. Cornelissen and R. Vazquez-Duhalt, *Enzyme Microb. Technol.*, 2014, **60**, 24–31.
61 M. Comellas-Aragonès, H. Engelkamp, V. I. Claessen, N. A. J. M. Sommerdijk, A. E. Rowan, P. C. M. Christianen, J. C. Maan, B. J. M. Verduin, J. J. L. M. Cornelissen and R. J. M. Nolte, *Nat. Nanotechnol.*, 2007, **2**, 635–639.
62 A. Liu, M. Verwegen, M. V. de Ruiter, S. J. Maassen, C. H. H. Traulsen and J. J. L. M. Cornelissen, *J. Phys. Chem. B*, 2016, **120**, 6352–6357.
63 A. Nuñez-Rivera, P. Fournier, D. Arellano, A. Hernandez, R. Vazquez-Duhalt and R. Cadena-Nava, *Beilstein J. Nanotechnol.*, 2020, **11**, 372–382.
64 K. Chauhan, C. N. Olivares-Medina, M. V. Villagrana-Escareño, K. Juárez-Moreno, R. D. Cadena-Nava, A. G. Rodríguez-Hernández and R. Vazquez-Duhalt, *ChemMedChem*, 2022, **17**, e202200384.
65 J. D. Fiedler, S. D. Brown, J. L. Lau and M. G. Finn, *Angew. Chem., Int. Ed.*, 2010, **49**, 9648–9651.
66 T. O. Paiva, A. Schneider, L. Bataille, A. Chovin, A. Anne, T. Michon, C. Wege and C. Demaille, *Nanoscale*, 2022, **14**, 875–889.
67 T. Inoue, M.-a Kawano, R.-u Takahashi, H. Tsukamoto, T. Enomoto, T. Imai, K. Kataoka and H. Handa, *J. Biotechnol.*, 2008, **134**, 181–192.
68 S. M. DePorter and B. R. McNaughton, *Bioconjugate Chem.*, 2014, **25**, 1620–1625.
69 L. Loo, R. H. Guenther, V. R. Basnayake, S. A. Lommel and S. Franzen, *J. Am. Chem. Soc.*, 2006, **128**, 4502–4503.
70 A. de la Escosura, M. Verwegen, F. D. Sikkema, M. Comellas-Aragonès, A. Kirilyuk, T. Rasing, R. J. M. Nolte and J. J. L. M. Cornelissen, *Chem. Commun.*, 2008, 1542–1544.
71 T. Douglas and M. Young, *Nature*, 1998, **393**, 152–155.
72 F. D. Sikkema, M. Comellas-Aragonès, R. G. Fokkink, B. J. M. Verduin, J. J. L. M. Cornelissen and R. J. M. Nolte, *Org. Biomol. Chem.*, 2007, **5**, 54–57.
73 W. E. Running, P. Ni, C. C. Kao and J. P. Reilly, *J. Mol. Biol.*, 2012, **423**, 79–95.
74 R. D. Cadena-Nava, Y. Hu, R. F. Garmann, B. Ng, A. N. Zelikin, C. M. Knobler and W. M. Gelbart, *J. Phys. Chem. B*, 2011, **115**, 2386–2391.
75 M. Comellas-Aragonès, A. de la Escosura, A. J. Dirks, A. van der Ham, A. Fusté-Cuñé, J. J. L. M. Cornelissen and R. J. M. Nolte, *Biomacromolecules*, 2009, **10**, 3141–3147.
76 C. Chen, M.-C. Daniel, Z. T. Quinkert, M. De, B. Stein, V. D. Bowman, P. R. Chipman, V. M. Rotello, C. C. Kao and B. Dragnea, *Nano Lett.*, 2006, **6**, 611–615.
77 J. Sun, C. DuFort, M.-C. Daniel, A. Murali, C. Chen, K. Gopinath, B. Stein, M. De, V. M. Rotello, A. Holzenburg, C. C. Kao and B. Dragnea, *Proc. Natl. Acad. Sci. U. S. A.*, 2007, **104**, 1354–1359.
78 D. P. Patterson, P. E. Prevelige and T. Douglas, *ACS Nano*, 2012, **6**, 5000–5009.
79 R. F. Garmann, M. Comas-Garcia, C. M. Knobler and W. M. Gelbart, *Acc. Chem. Res.*, 2016, **49**, 48–55.
80 J. D. Fiedler, C. Higginson, M. L. Hovlid, A. A. Kislukhin, A. Castillejos, F. Manzenrieder, M. G. Campbell, N. R. Voss, C. S. Potter, B. Carragher and M. G. Finn, *Biomacromolecules*, 2012, **13**, 2339–2348.
81 G. P. Lomonossoff and C. Wege, *Adv. Virus Res.*, 2018, **102**, 149–176.
82 C. Koch, F. J. Eber, C. Azucena, A. Förste, S. Walheim, T. Schimmel, A. M. Bittner, H. Jeske, H. Gliemann, S. Eiben, F. C. Geiger and C. Wege, *Beilstein J. Nanotechnol.*, 2016, **7**, 613–629.
83 K. A. Dowd and T. C. Pierson, *Annu. Rev. Virol.*, 2018, **5**, 185–207.

84 F. Tama and C. L. Brooks, *J. Mol. Biol.*, 2002, **318**, 733–747.
85 N. Tasneem, T. N. Szyszka, E. N. Jenner and Y. H. Lau, *ACS Nano*, 2022, **16**, 8540–8556.
86 L. S. R. Adamson, N. Tasneem, M. P. Andreas, W. Close, E. N. Jenner, T. N. Szyszka, R. Young, L. C. Cheah, A. Norman, H. I. MacDermott-Opeskin, M. L. O'Mara, F. Sainsbury, T. W. Giessen and Y. H. Lau, *Sci. Adv.*, 2022, **8**, eabl7346.
87 P. Kraj, N. D. Hewagama and T. Douglas, *Virology*, 2023, **580**, 50–60.
88 B. D. Wilts, I. A. Schaap and C. F. Schmidt, *Biophys. J.*, 2015, **108**, 2541–2549.
89 J. Witz and F. Brown, *Arch. Virol.*, 2001, **146**, 2263–2274.
90 R. Perera and R. J. Kuhn, *Curr. Opin. Microbiol.*, 2008, **11**, 369–377.
91 J. E. Voss, M.-C. Vaney, S. Duquerroy, C. Vonrhein, C. Girard-Blanc, E. Crublet, A. Thompson, G. Bricogne and F. A. Rey, *Nature*, 2010, **468**, 709–712.
92 T. Matsui, H. Tsuruta and J. E. Johnson, *Biophys. J.*, 2010, **98**, 1337–1343.
93 R. F. Bruinsma, G. J. L. Wuite and W. H. Roos, *Nat. Rev. Phys.*, 2021, **3**, 76–91.
94 J. K. Marzinek, R. G. Huber and P. J. Bond, *Curr. Opin. Struct. Biol.*, 2020, **61**, 146–152.
95 T. Li, Q. Jiang, J. Huang, C. M. Aitchison, F. Huang, M. Yang, G. F. Dykes, H.-L. He, Q. Wang, R. S. Sprick, A. I. Cooper and L.-N. Liu, *Nat. Commun.*, 2020, **11**, 5448.
96 W. H. Roos, I. L. Ivanovska, A. Evilevitch and G. J. L. Wuite, *Cell. Mol. Life Sci.*, 2007, **64**, 1484.
97 R. Gao, H. Tan, S. Li, S. Ma, Y. Tang, K. Zhang, Z. Zhang, Q. Fan, J. Yang, X.-E. Zhang and F. Li, *Proc. Natl. Acad. Sci. U. S. A.*, 2022, **119**, e2104964119.
98 J. F. Ek-Vitorin and J. M. Burt, *Biochim. Biophys. Acta, Biomembr.*, 2013, **1828**, 51–68.
99 I. Aprahamian, *ACS Cent. Sci.*, 2020, **6**, 347–358.
100 R. J. Kuhn, K. A. Dowd, C. Beth Post and T. C. Pierson, *Virology*, 2015, **479–480**, 508–517.
101 C. Luo, L. He, F. Chen, T. Fu, P. Zhang, Z. Xiao, Y. Liu and W. Tan, *Cell Rep. Phys. Sci.*, 2021, **2**, 2.
102 A. Lošdorfer Božič, A. Šiber and R. Podgornik, *J. Biol. Phys.*, 2012, **38**, 657–671.
103 R. Konecny, J. Trylska, F. Tama, D. Zhang, N. A. Baker, C. L. Brooks III and J. A. McCammon, *Biopolymers*, 2006, **82**, 106–120.
104 A. Liu, C. H. H. Traulsen and J. J. L. M. Cornelissen, *ACS Catal.*, 2016, **6**, 3084–3091.
105 Y. Azuma, D. L. V. Bader and D. Hilvert, *J. Am. Chem. Soc.*, 2018, **140**, 860–863.
106 Y. Wang and T. Douglas, *Acc. Chem. Res.*, 2022, **55**, 1349–1359.
107 M. Uchida, E. Manzo, D. Echeveria, S. Jiménez and L. Lovell, *Curr. Opin. Virol.*, 2022, **52**, 250–257.
108 D. N. Silverman, *Biochim. Biophys. Acta, Bioenerg.*, 2000, **1458**, 88–103.
109 N. G. Léonard, R. Dhaoui, T. Chantarojsiri and J. Y. Yang, *ACS Catal.*, 2021, **11**, 10923–10932.
110 D. Zakaszewski, L. Koziej, J. Pankowski, V. V. Malolan, N. Gämperli, J. G. Heddle, D. Hilvert and Y. Azuma, *J. Mater. Chem. B*, 2023, **11**, 6540–6546.
111 J. Huang, Q. Jiang, M. Yang, G. F. Dykes, S. L. Weetman, W. Xin, H.-L. He and L.-N. Liu, *Biomacromolecules*, 2022, **23**, 4339–4348.
112 H. K. Waghwani and T. Douglas, *J. Mater. Chem. B*, 2021, **9**, 3168–3179.
113 S. J. Maassen, P. van der Schoot and J. J. L. M. Cornelissen, *Small*, 2018, **14**, 1802081.
114 H. J. Muhren and P. van der Schoot, *J. Phys. Chem. B*, 2023, **127**, 2160–2168.
115 K. Chauhan, A. Zárate-Romero, P. Sengar, C. Medrano and R. Vazquez-Duhalt, *ChemCatChem*, 2021, **13**, 3732–3748.
116 Y. Zhang and H. Hess, *ACS Catal.*, 2017, **7**, 6018–6027.
117 G. Ölçücü, O. Klaus, K.-E. Jaeger, T. Drepper and U. Krauss, *ACS Sustainable Chem. Eng.*, 2021, **9**, 8919–8945.
118 Y. Zhang and H. Hess, *ACS Cent. Sci.*, 2019, **5**, 939–948.
119 Y.-Q. Zhang, T.-T. Feng, Y.-F. Cao, X.-Y. Zhang, T. Wang, M. R. Huanca Nina, L.-C. Wang, H.-L. Yu, J.-H. Xu, J. Ge and Y.-P. Bai, *ACS Catal.*, 2021, **11**, 10487–10493.
120 C. Schmid-Dannert and F. López-Gallego, *Curr. Opin. Chem. Biol.*, 2019, **49**, 97–104.
121 I. V. Gopich, *J. Phys. Chem. B*, 2021, **125**, 2061–2073.
122 I. Wheeldon, S. D. Minteer, S. Banta, S. C. Barton, P. Atanassov and M. Sigman, *Nat. Chem.*, 2016, **8**, 299–309.
123 B. Dong, N. Mansour, Y. Pei, Z. Wang, T. Huang, S. L. Filbrun, M. Chen, X. Cheng, M. Pruski, W. Huang and N. Fang, *J. Am. Chem. Soc.*, 2020, **142**, 13305–13309.
124 Q. Wei, S. He, J. Qu and J. Xia, *Bioconjugate Chem.*, 2020, **31**, 2413–2420.
125 C. Mateo, J. M. Palomo, G. Fernandez-Lorente, J. M. Guisan and R. Fernandez-Lafuente, *Enzyme Microb. Technol.*, 2007, **40**, 1451–1463.
126 A. Basso, P. Braiuca, C. Ebert, L. Gardossi and P. Linda, *J. Chem. Technol. Biotechnol.*, 2006, **81**, 1626–1640.
127 P. J. Halling, R. V. Ulijn and S. L. Flitsch, *Curr. Opin. Biotechnol*, 2005, **16**, 385–392.
128 C. Koch, K. Wabbel, F. J. Eber, P. Krolla-Sidenstein, C. Azucena, H. Gliemann, S. Eiben, F. Geiger and C. Wege, *Front. Plant Sci.*, 2015, **6**, 1137.
129 A. A. A. Aljabali, J. E. Barclay, N. F. Steinmetz, G. P. Lomonossoff and D. J. Evans, *Nanoscale*, 2012, **4**, 5640–5645.
130 F. C. Geiger, F. J. Eber, S. Eiben, A. Mueller, H. Jeske, J. P. Spatz and C. Wege, *Nanoscale*, 2013, **5**, 3808–3816.
131 R. Otten, L. Liu, L. R. Kenner, M. W. Clarkson, D. Mavor, D. S. Tawfik, D. Kern and J. S. Fraser, *Nat. Commun.*, 2018, **9**, 1314.
132 Y. R. Yang, J. Fu, S. Wootten, X. Qi, M. Liu, H. Yan and Y. Liu, *ChemBioChem*, 2018, **19**, 212–216.
133 L. Schoonen and J. C. M. van Hest, *Adv. Mater.*, 2016, **28**, 1109–1128.
134 M. B. Quin, K. K. Wallin, G. Zhang and C. Schmidt-Dannert, *Org. Biomol. Chem.*, 2017, **15**, 4260–4271.
135 O. González-Davis, K. Chauhan, S.-J. Zapian-Merino and R. Vazquez-Duhalt, *Int. J. Biol. Macromol.*, 2020, **146**, 415–421.

136 S.-T. Wang, B. Minevich, J. Liu, H. Zhang, D. Nykypanchuk, J. Byrnes, W. Liu, L. Bershadsky, Q. Liu, T. Wang, G. Ren and O. Gang, *Nat. Commun.*, 2021, **12**, 3702.
137 Q. Liu, Y. Zhou, A. Shaukat, Z. Meng, D. Kyllönen, I. Seitz, D. Langerreiter, K. Kuntze, A. Priimagi, L. Zheng and M. A. Kostiainen, *Angew. Chem., Int. Ed.*, 2023, **62**, e202303880.
138 J. S. Liu and Z. J. Gartner, *Trends Cell Biol.*, 2012, **22**, 683–691.
139 S. Yang, Y. Wang, Q. Wang, F. Li and D. Ling, *Chem. Biomed. Imaging*, 2023, **1**, 340–355.
140 T. G. W. Edwardson, M. D. Levasseur, S. Tetter, A. Steinauer, M. Hori and D. Hilvert, *Chem. Rev.*, 2022, **122**, 9145–9197.
141 R. Sun and S. Lim, *Eng. Biol.*, 2021, **5**, 35–42.
142 E. Selivanovitch, M. Uchida, B. Lee and T. Douglas, *ACS Nano*, 2021, **15**, 15687–15699.
143 B. Maity, S. Abe and T. Ueno, *Nat. Commun.*, 2017, **8**, 14820.
144 M. Uchida, B. LaFrance, C. C. Broomell, P. E. Prevelige Jr. and T. Douglas, *Small*, 2015, **11**, 1562–1570.
145 A. Liu, M. V. de Ruiter, W. Zhu, S. J. Maassen, L. Yang and J. J. L. M. Cornelissen, *Adv. Funct. Mater.*, 2018, **28**, 1801574.
146 C. Xue, Q. Han, Y. Wang, J. Wu, T. Wen, R. Wang, J. Hong, X. Zhou and H. Jiang, *Biosens. Bioelectron.*, 2013, **49**, 199–203.
147 Q. Zhu, H. Yang, J. Luo, H. Huang, L. Fang, J. Deng, C. Li, Y. Li, T. Zeng and J. Zheng, *Anal. Chim. Acta*, 2021, **1142**, 127–134.
148 Y. Ji, Y. Lin and Y. Qiao, *J. Am. Chem. Soc.*, 2023, **145**, 12576–12585.
149 V. Liljeström, J. Mikkilä and M. A. Kostiainen, *Nat. Commun.*, 2014, **5**, 4445.
150 K. McCoy, M. Uchida, B. Lee and T. Douglas, *ACS Nano*, 2018, **12**, 3541–3550.
151 A. Jain and R. Zoncu, *Mol. Metab.*, 2022, **60**, 101481.
152 S. Wang, B. Binevich, J. Liu, H. Zhang, D. Nykypanchuk, J. Byrnes, W. Liu, L. Bershadsky, Q. Liu, T. Wang, G. Ren and O. Gang, *Nat. Commun.*, 2021, **12**, 3702.
153 C. Gu, H. Chen, Y. Wang, T. Zhang, H. Wang and G. Zhao, *Chem. – Eur. J.*, 2020, **26**, 3016–3021.
154 A. Korpi, C. Ma, K. Liu, Nonappa, A. Herrmann, O. Ikkala and M. A. Kostiainen, *ACS Macro Lett.*, 2018, **7**, 318–323.
155 Y. Wang and T. Douglas, *Curr. Opin. Colloid Interface Sci.*, 2021, **51**, 101395.
156 A. O'Neil, P. E. Prevelige and T. Douglas, *Biomater. Sci.*, 2013, **1**, 881–886.
157 O. González-Davis, M. V. Villagrana-Escareño, M. A. Trujillo, P. Gama, K. Chauhan and R. Vazquez-Duhalt, *Virology*, 2023, **580**, 73–87.
158 F. Sainsbury and N. Steinmetz, *Virology*, 2023, **581**, 56–57.
159 P. Gama, R. D. Cadena-Nava, K. Juarez-Moreno, J. Pérez-Robles and R. Vazquez-Duhalt, *ChemMedChem*, 2021, **16**, 1438–1445.
160 T. Kwon, J. S. Ra, S. Lee, I.-J. Baek, K. W. Khim, E. A. Lee, E. K. Song, D. Otarbayev, W. Jung, Y. H. Park, M. Wie, J. Bae, H. Cheng, J. H. Park, N. Kim, Y. Seo, S. Yun, H. E. Kim, H. E. Moon, S. H. Paek, T. J. Park, Y. U. Park, H. Rhee, J. H. Choi, S. W. Cho and K. Myung, *Proc. Natl. Acad. Sci. U. S. A.*, 2022, **119**, e2103532119.
161 E. J. Lee, N. K. Lee and I.-S. Kim, *Adv. Drug Delivery Rev.*, 2016, **106**, 157–171.
162 K. Chauhan, P. Sengar, K. Juarez-Moreno, G. A. Hirata and R. Vazquez-Duhalt, *J. Colloid Interface Sci.*, 2020, **580**, 365–376.
163 Y. Zhang, H. Cui, R. Zhang, H. Zhang and W. Huang, *Adv. Sci.*, 2021, **8**, 2101454.
164 E. J. Hartzell, R. M. Lieser, M. O. Sullivan and W. Chen, *ACS Nano*, 2020, **14**, 12642–12651.
165 K. Chauhan, J. M. Hernandez-Meza, A. G. Rodríguez-Hernández, K. Juarez-Moreno, P. Sengar and R. Vazquez-Duhalt, *J. Nanobiotechnol.*, 2018, **16**, 17.
166 J. L. Mejía-Méndez, R. Vazquez-Duhalt, L. R. Hernández, E. Sánchez-Arreola and H. Bach, *Int. J. Mol. Sci.*, 2022, **23**, 8579.
167 D. F. M. Vervoort, R. Heiringhoff, S. B. P. E. Timmermans, M. H. M. E. van Stevendaal and J. C. M. van Hest, *Bioconjugate Chem.*, 2021, **32**, 958–963.
168 T. Zhao, Y. Cai, Y. Jiang, X. He, Y. Wei, Y. Yu and X. Tian, *Signal Transduction Targeted Ther.*, 2023, **8**, 283.
169 D. Cardinale, N. Carette and T. Michon, *Trends Biotechnol.*, 2012, **30**, 369–376.
170 D. P. Patterson, B. Schwarz, R. S. Waters, T. Gedeon and T. Douglas, *ACS Chem. Biol.*, 2014, **9**, 359–365.
171 S. Speer, W. Zheng, X. Jiang, I. Chu, A. Guseman, M. Liu, G. Pielak and C. Li, *Proc. Natl. Acad. Sci. U. S. A.*, 2021, **118**, e2019918118.
172 D. P. Patterson, B. Schwarz, K. El-Boubbou, J. van der Oost, P. E. Prevelige and T. Douglas, *Soft Matter*, 2012, **8**, 10158–10166.
173 H. Karoui, P. S. Patwal, B. V. V. S. Pavan Kumar and N. Martin, *Front. Mol. Biosci.*, 2022, **9**, 880525.
174 Y. Deng, T. Wu, X. Chen, Y. Chen, Y. Fei, Y. Liu, Z. Chen, H. Xing and Y. Bai, *J. Am. Chem. Soc.*, 2023, **145**, 1262–1272.
175 J. H. Swisher, L. Jibril, S. H. Petrosko and C. A. Mirkin, *Nat. Rev. Mater.*, 2022, **7**, 428–448.
176 H. K. Waghwani, M. Uchida, C.-Y. Fu, B. LaFrance, J. Sharma, K. McCoy and T. Douglas, *Biomacromolecules*, 2020, **21**, 2060–2072.
177 O. Tagit, M. V. de Ruiter, M. Brasch, Y. Ma and J. J. L. M. Cornelissen, *RSC Adv.*, 2017, **7**, 38110–38118.
178 K. R. Kim, A. S. Lee, S. M. Kim, H. R. Heo and C. S. Kim, *Front. Bioeng. Biotechnol.*, 2023, **10**, 1106767.
179 X. Sun and Z. Cui, *Adv. Ther.*, 2020, **3**, 1900194.

